

Tunable graphene band gaps from superstrate-mediated interactions

J. P. Hague

Department of Physical Sciences, The Open University, Walton Hall, Milton Keynes, MK7 6AA, United Kingdom

(Received 1 June 2011; revised manuscript received 9 September 2011; published 27 October 2011)

A theory is presented for the strong enhancement of graphene-on-substrate band gaps by attractive interactions mediated through phonons in a polarizable superstrate. It is demonstrated that gaps of up to 1 eV can be formed for experimentally achievable values of electron-phonon coupling and phonon frequency. Gap enhancements range between factors of 1 to 4, indicating possible benefits to graphene electronics through greater band-gap control for digital applications, lasers, light-emitting diodes, and photovoltaics through the relatively simple application of polarizable materials such as SiO₂ and Si₃N₄.

DOI: [10.1103/PhysRevB.84.155438](https://doi.org/10.1103/PhysRevB.84.155438)

PACS number(s): 73.22.Pr

I. INTRODUCTION

A key goal for graphene research is the development of applications which require substantial band gaps, such as digital transistors. Graphene monolayers have zero band gaps, but small gaps have been observed when graphene is placed on substrates such as SiC (250 meV) (Ref. 1) and gold on ruthenium (200 meV) (Ref. 2) and predicted for graphene on boron nitride (100 meV).³ A technique for enhancing these gaps up to the 1-eV order of magnitude seen in silicon is crucial to the development of digital electronics. Moreover, the ability to make spatially dependent changes to the gap of a semiconducting material should open a route to new electronic devices and applications, and the availability of strongly tunable gaps is important to the development of laser diodes, light-emitting diodes (LEDs), photovoltaics, heterojunctions, and photodetectors.

Here, I investigate gap-enhancement effects due to interactions mediated through superstrates placed on graphene systems in which a gap has been opened with a modulated potential. For example, sublattice symmetry breaking has been suggested as the gap-opening mechanism for the graphene-on-ruthenium system.² The specific aim is to establish if the small gap size of, e.g., graphene on ruthenium can be increased using attractive electron-phonon coupling to vibrations in a strongly polarizable superstrate. In low-dimensional materials, strong effective electron-electron interactions can be induced via the interaction between electrons confined to a plane and phonons in a neighboring layer that is polarizable.⁴ In the context of carbon systems, experiment has shown that electron-phonon interactions between carbon nanotubes and SiO₂ substrates have strong effects on transport properties,⁵ and theory has shown that similar interactions account for the transport properties of graphene on polarizable substrates.⁶

Besides graphene on substrates, several alternative options have been put forward to generate gaps in graphene. McCann and Falco^{7,8} proposed that bilayer graphene develops a gap when it is gated with an electric field, and the bilayer graphene gap has been observed experimentally by Ohta *et al.* using angle-resolved photoemission spectroscopy⁹ and by Zhang *et al.* using infrared spectroscopy.¹⁰

Electron confinement in quasi-one-dimensional structures has also been put forward as a solution to the generation of band gaps. Graphene nanoribbons with certain edge orientations

were theoretically hypothesized some time ago to possess gaps,^{11,12} and it has been shown using *ab initio* calculations that reduction of the nanoribbon width can lead to substantial gap sizes due to electron confinement although for gap sizes on the order of 1 eV, very narrow nanoribbons with widths on the order of 10 Å are required. An increase in nanoribbon gaps up to around 300 meV due to electron confinement has been measured by Han *et al.*¹³ although the width variation of the ribbons is large. Recent developments have allowed for the manufacture of high-quality nanoribbons via the unzipping of nanotubes,¹⁴ and theoretical predictions have been confirmed experimentally with a measured gap of 23.8 ± 3.2 meV for an (8,1) nanoribbon.¹⁵

A more extreme solution involves changing the chemistry of graphene monolayers. The generation of large band gaps in graphene on the order of several eV has been hypothesized for chemical modification with hydrogen (graphane) (Refs. 16 and 17) and fluorine (fluorographene).¹⁸ While forms of graphane¹⁹ and fluorographene²⁰ have been manufactured and hints of band gaps have been found, there is currently no consensus on the size of these band gaps as it is difficult to obtain even coverage of the hydrogen or fluorine. Also, it is likely that the wide band gaps are too large for many digital applications. Finally, I briefly mention that graphene on some substrates forms moiré patterns, which also lead to a modified electronic structure.²¹

This paper is organized as follows. A model for graphene sandwiched between a dielectric superstrate and a gap-opening substrate is introduced in Sec. II. In Sec. III results from Hartree-Fock theory in the high-phonon-frequency limit are presented. Perturbation theory and results for low phonon frequency are presented in Sec. IV. A summary and outlook can be found in Sec. V.

II. MODEL

A model Hamiltonian for the electronic properties of graphene on a substrate modified by the presence of a superstrate should have at least three components. The first is a mechanism for electrons to move through the material, the second is an electron-phonon interaction, and the third is a static potential to describe symmetry breaking between graphene sublattices by the substrate. The presence of superstrates also opens the possibility of long-range electron-phonon interactions. As such, a model Hamiltonian for graphene on a

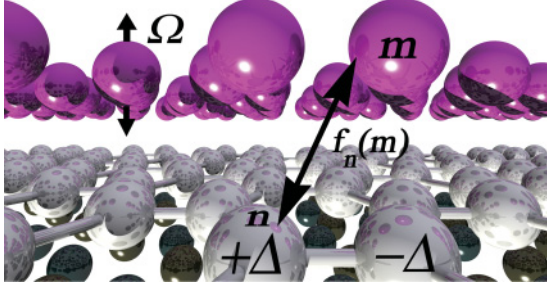


FIG. 1. (Color online) Graphene-substrate-superstrate system annotated with interactions and sublattices. Electron-phonon interactions between the graphene layer and superstrate are poorly screened, and large interactions of strength $f_n(m)$ are possible. Ions in the superstrate oscillate with frequency Ω . A sites have energy $+\Delta$ and B sites $-\Delta$ due to the substrate. Atoms in the graphene sheet are indexed with vector \mathbf{n} and ions in the superstrate with \mathbf{m} .

substrate has the form,

$$H = -t \sum_{(n,n')\sigma} (a_{n\sigma}^\dagger c_{n'\sigma} + c_{n'\sigma}^\dagger a_{n\sigma}) - \sum_{nm\sigma} f_n(m) n_{n\sigma} \xi_m + \sum_m \hbar \Omega (N_m + 1/2) + \sum_{n\sigma} \Delta_n n_{n\sigma}. \quad (1)$$

The interactions between electrons in a graphene monolayer and polarizable ions in the superstrate are shown schematically in Fig. 1. The first term in the Hamiltonian describes the kinetic energy of tight-binding electrons, hopping in the graphene monolayer with amplitude t , written in momentum space as $\sum_{\mathbf{k}} (\phi_{\mathbf{k}} a_{\mathbf{k}}^\dagger c_{\mathbf{k}} + \phi_{\mathbf{k}}^* c_{\mathbf{k}}^\dagger a_{\mathbf{k}})$, where $\phi_{\mathbf{k}} = -t \sum_i \exp(i\mathbf{k} \cdot \delta_i)$ and δ_i are the nearest-neighbor vectors from graphene A to B sites [$\delta_1 = a(1, \sqrt{3})/2$, $\delta_2 = a(1, -\sqrt{3})/2$, and $\delta_3 = (-a, 0)$]. Electrons are created on graphene A sites with the operator a_n^\dagger and B sites with c_n^\dagger , and the vectors \mathbf{n} are to atoms in the plane.

The next term in the Hamiltonian describes the electron-phonon interaction, which has the momentum space form $\sum_{\mathbf{k}q} g_{\mathbf{k}q} [c_{\mathbf{k}-q}^\dagger c_{\mathbf{k}} (d_q^\dagger + d_{-q}) + a_{\mathbf{k}-q}^\dagger a_{\mathbf{k}} (b_q^\dagger + b_{-q})] + \sum_{\mathbf{k}q} \tilde{g}_{\mathbf{k}q} [a_{\mathbf{k}-q}^\dagger a_{\mathbf{k}} (d_q^\dagger + d_{-q}) + c_{\mathbf{k}-q}^\dagger c_{\mathbf{k}} (b_q^\dagger + b_{-q})]$. Phonons are created in the superstrate above A sites with b_m^\dagger and above the B sublattice with d_m^\dagger , so the displacement $\xi_m \propto (b_m^\dagger + d_m^\dagger)$ for A sites. The interaction strength $f_m(\mathbf{n}) = \kappa / [(\mathbf{m} - \mathbf{n})^2 + 1]^{3/2}$ has a classic Fröhlich form (where κ is a coupling constant). The effective phonon-mediated interaction between electrons can be characterized by the function $\Phi(\mathbf{n}, \mathbf{n}') = \sum_m f_m(\mathbf{n}) f_m(\mathbf{n}')$. A complication of this Hamiltonian is that a basis of two atoms is needed to represent the honeycomb lattice, which is the reason for the two interactions, g and \tilde{g} . For local electron-phonon coupling, \tilde{g} vanishes, and g becomes momentum independent. For simplicity, I study this simplified version of the electron-phonon Hamiltonian²² in which the effective interaction is approximated as a Holstein model that has the local interaction $\Phi(\mathbf{n}, \mathbf{n}') = \delta_{\mathbf{n}, \mathbf{n}'}$. The third term represents the energy of phonons with frequency Ω , where N_m is the number operator for phonons. It is appropriate to mention the effect of the electron-phonon interaction on suspended graphene, which simply leads to renormalizations of phonon and electron modes.^{22,23}

The Fröhlich form for the electron-phonon interaction has been demonstrated experimentally for carbon nanotubes on SiO_2 ,⁵ and it has been established as the main scattering mechanism for graphene on SiO_2 .⁶ With weak electron-phonon coupling, the effects of Holstein and Fröhlich interactions are qualitatively similar on two-dimensional lattices,²⁴ and the Holstein form is used throughout this paper. It is worth noting that there may be quantitative changes to the results presented in this paper for longer-range interactions.

For completeness, I briefly discuss an alternative class of electron-phonon interaction in which the phonon motion couples to the electron hopping, leading to a Su-Schrieffer-Heeger (SSH)-style interaction, which can lead to dimerization (and could act against the mechanism used here).²⁵ To have a strong SSH interaction, a material must be very flexible (e.g., the SSH model is very good for describing polymers). Here, since the graphene is sandwiched between two other materials, the material will be held rigid, and in-plane SSH interactions are expected to be much smaller than the Holstein-style interaction considered here.

I also note that there may be some modulation of the strength of the electron-phonon interaction due to incommensurability of the superstrate. The effects of this incommensurability are straightforward to estimate in one dimension by computing the sum $\Phi(\mathbf{n}, \mathbf{n}') = \sum_m f_m(\mathbf{n}) f_m(\mathbf{n}')$ for values of \mathbf{n} intermediate to the lattice points. It is found that the interaction strength varies by around $\pm 8\%$ of the average value if the superstrate is incommensurate. It is not expected that modulations of this magnitude will qualitatively change the results presented here.

To complete the model of the graphene-substrate-superstrate system, the final term in the Hamiltonian describes interaction between electrons and a static potential Δ_n induced by the substrate. In particular, a modulated potential where A sites have energy Δ and B sites $-\Delta$ leads to the breaking of the symmetry between A and B sites and gives rise to a gap. In the following, I examine the effects of electron-phonon interaction on this gap. The effect of phonons on substrate-induced gaps has not previously been studied, and as I show, the implication for the gap is significant.

III. HIGH PHONON FREQUENCY

To illustrate the core physical content of the model, I initially study the high-phonon-frequency limit in which a Lang-Firsov canonical transformation can be used to derive an effective Hubbard Hamiltonian²⁶

$$H = \sum_{\mathbf{k}} \phi_{\mathbf{k}}' a_{\mathbf{k}\sigma}^\dagger c_{\mathbf{k}\sigma} + \text{H.c.} + \sum_i U' n_{i\uparrow} n_{i\downarrow} + \sum_i \Delta_i n_i, \quad (2)$$

where $U' = U - 2t\lambda$, $|\phi_{\mathbf{k}}'|^2 = 3t^2 + t'^2 [2 \cos(k_y \sqrt{3}) + 4 \cos(k_y \sqrt{3}/2) \cos(3k_x/2)]$ is the dispersion for the graphene lattice, $t' = t \exp(-t\lambda/\Omega)$, and $\lambda = \Phi(0,0)/2tM\Omega^2$ is the dimensionless electron-phonon coupling that is expected to be smaller than unity (M is the ion mass). A local Coulomb repulsion U has been included for completeness although the effects of this in the graphene monolayer are limited to renormalization of the electron bands since no phase transition (to, e.g., a Mott insulator) is measured, avoiding the need for more complicated treatments of the Coulomb

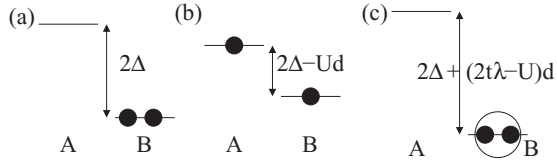


FIG. 2. Schematic of the physical processes highlighted in the high-phonon-frequency limit. (a) The modulated potential with magnitude Δ opens a gap. (b) The effect of Coulomb repulsion is to stop both electrons occupying the same site, effectively closing the gap. (c) The attractive phonon-mediated electronic interaction with coupling constant λ pulls electrons to the same site and reduces the hopping, effectively enhancing the gap. d is the difference in electron occupation between sites A and B.

repulsion. Figure 2 shows the basic physical processes that lead to gap modification in graphene-on-substrate systems in the high-phonon-frequency limit. Figure 2(a) shows the gap induced from the modulated potential where electrons prefer to sit on the lower-energy site B. If sufficient Coulomb repulsion is applied, electrons occupy different sites, and this leads to an effective lowering of the gap as shown in Fig. 2(b). Contrary to this, an electron-phonon interaction leads to lower energies when electrons are on the same site and also tends to decrease the effective hopping, which is expected to increase the gap [see Fig. 2(c)].

For weak coupling, the Hamiltonian may be decoupled using the standard Hartree-Fock scheme, i.e., the interacting Hamiltonian on A sites is decoupled as $H_A \approx U' \langle n_{iA\uparrow} \rangle n_{iA\downarrow} + U' \langle n_{iA\downarrow} \rangle n_{iA\uparrow} - U' \langle n_{iA\uparrow} \rangle \langle n_{iA\downarrow} \rangle$ and the interacting Hamiltonian on B sites is decoupled in a similar way. A mean-field solution is then taken with $\langle n_{iA} \rangle = n + d$ and $\langle n_{iB} \rangle = n - d$, where n is the mean occupation and d the deviation from that occupation. In the following, the system is half filled. Minimizing the total energy with respect to d , a gap equation for d is obtained,

$$d = -\frac{1}{V_{BZ}} \int d^2\mathbf{k} \frac{(Ud/2 - t\lambda d + \Delta)/2}{\sqrt{(\phi'_k)^2 + \Delta^2}}, \quad (3)$$

where $\Delta' = (U - 2t\lambda)d/2 + \Delta$ is the effective bandwidth once interactions are taken into account and V_{BZ} is the Brillouin zone volume. This may be solved by using a binary search. The results for Δ' can be seen in Fig. 3. The effect of increased Coulomb repulsion is a small decrease in the effective gap. The effect of the increased electron-phonon coupling λ is far more dramatic, and the gap increases are seen for all λ at any U value. I note that the enhancement increases as the bare gap Δ decreases. Crucially, enhancement factors of ~ 4 can be seen for medium-sized λ , which could increase the moderate gaps seen experimentally in graphene-on-substrate systems to the ~ 1 -eV-gap sizes of silicon and germanium with the caveat that changes in the form of the electron-phonon coupling could quantitatively alter this result. By changing the form of the superstrate or substrate, significant control could be exercised over the graphene band gap.

IV. LOW PHONON FREQUENCY

Given the large gap enhancement in the high-phonon-frequency limit, it is appropriate to examine whether or not

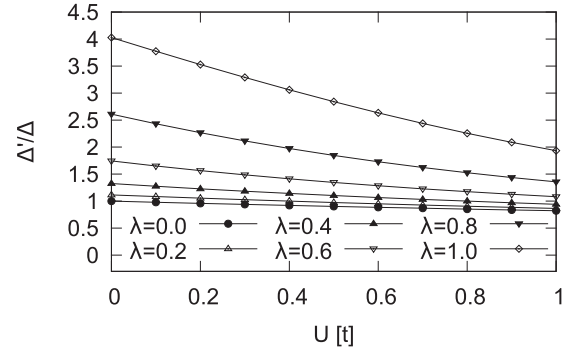


FIG. 3. Enhancement of the substrate-induced graphene band gap in the antiadiabatic (high-phonon-frequency) limit. Enhancement factors of ~ 4 can be seen for medium-sized λ . Here, parameters $T = 0$, $\hbar\Omega = t$, and $\Delta = 0.1t$ are used. The results here are illustrative of the core physics, and solutions of full Eliashberg-style equations for physically realistic parameters are shown in Fig. 4.

the enhancement is present at low phonon frequency. It is not obvious that the intuitive gap enhancement seen at high phonon frequencies should still occur at low frequencies where retardation effects can lead to large pairs that are not localized. For low phonon frequency and weak coupling, low-order perturbation theory can be applied. I derive a set of self-consistent equations assuming the following ansatz for the self-energy,

$$\Sigma(i\omega_n) \approx \begin{pmatrix} i\omega_n(1 - Z_n) + \bar{\Delta}_n & 0 \\ 0 & i\omega_n(1 - Z_n) - \bar{\Delta}_n \end{pmatrix}.$$

Here, the momentum-independent form of the ansatz (local approximation) is reasonable because of localization by the modulated potential Δ and the electron-phonon interaction. Off-diagonal terms are absent because they do not feature in the lowest-order perturbation theory. The quasiparticle weight Z_n is shorthand for $Z(i\omega_n)$, and $\bar{\Delta}_n$ is the gap function. Matsubara energies for bosonic quantities are $\omega_s = 2\pi k_B T s$ and for fermions are $\omega_n = 2\pi k_B T (n + 1/2)$, where T is the temperature and n and s are integers.

The noninteracting graphene Green function in the presence of a modulated potential has the form

$$\mathbf{G}_0^{-1}(\mathbf{k}, i\omega_n) = \begin{pmatrix} i\omega_n - \Delta & \phi_{\mathbf{k}}^* \\ \phi_{\mathbf{k}} & i\omega_n + \Delta \end{pmatrix}. \quad (4)$$

The full Green function can be established using Dyson's equation, $\mathbf{G}^{-1}(\mathbf{k}, i\omega_n) = \mathbf{G}_0^{-1}(\mathbf{k}, i\omega_n) - \Sigma(i\omega_n)$, leading to

$$\mathbf{G}^{-1}(\mathbf{k}, i\omega_n) = \begin{pmatrix} i\omega_n Z_n - \Delta - \bar{\Delta}_n & \phi_{\mathbf{k}}^* \\ \phi_{\mathbf{k}} & i\omega_n Z_n + \Delta + \bar{\Delta}_n \end{pmatrix}. \quad (5)$$

Substituting the expression for the Green function into the lowest-order contribution to the self-energy,

$$\Sigma_{ii}(\mathbf{k}, i\omega_n) = -Tt\lambda \sum_{i\omega_s} \int \frac{d^2\mathbf{q}}{V_{BZ}} G_{ii}(\mathbf{k} - \mathbf{q}, i\omega_{n-s}) d_0(\mathbf{q}, \omega_s). \quad (6)$$

Here, the phonon propagator $d_0(\mathbf{q}, \omega_s) = \Omega^2 / (\Omega^2 + \omega_s^2)$. The off-diagonal elements of the lowest-order self-energy are zero in the case of local interaction, so they do not feature in the ansatz. Since there is a modulated potential, it is necessary also to take into account the tadpole diagram (which has a contribution since the effects of the modulated potential cannot simply be absorbed into the chemical potential), leading to the following Eliashberg-style equations for $\bar{\Delta}_n$ and Z_n ,

$$\bar{\Delta}_n = 2t\lambda\delta n - t\lambda k_B T \sum_s \int d\epsilon \frac{D(\epsilon) \Delta'_{n-s} d_0(i\omega_s)}{\omega_{n-s}^2 Z_{n-s}^2 + \Delta'_{n-s}{}^2 + \epsilon^2}, \quad (7)$$

$$\delta n = k_B T \sum_n \int d\epsilon \frac{D(\epsilon) \Delta'_n}{\omega_n^2 Z_n^2 + \Delta_n'^2 + \epsilon^2}, \quad (8)$$

and

$$Z_n = 1 - \frac{t\lambda k_B T}{\omega_n} \sum_s \int d\epsilon \frac{D(\epsilon) \omega_{n-s} Z_{n-s} d_0(i\omega_s)}{\omega_{n-s}^2 Z_{n-s}^2 + \Delta'_{n-s}{}^2 + \epsilon^2}, \quad (9)$$

where δn is the difference between the density of electrons at sites A and B and the full gap is $\Delta'_n = \bar{\Delta}_n + \Delta$. Here, the density of states for graphene in the absence of a gap, $D(\epsilon)$ has the form given in Ref. 23. Note that these gap equations differ from those for a superconductor.

The equations may be solved self-consistently by performing a truncated sum on the Matsubara frequencies. The maximum Matsubara frequency was kept constant with the value $\omega_{\max} = 75t$, which is sufficiently large to ensure that asymptotic behavior of the gap function is achieved. The longest self-consistent solutions took around two weeks, increasing as $1/T$ and λ . The following parameters were chosen to match graphene with a modest bare gap on the order of magnitude seen in the systems discussed in the Introduction: $\Delta = 0.05t$, corresponding to a gap of around 280 meV, realistically achievable phonon energies of $\hbar\Omega = 0.01t = 28$ meV, $\lambda < 1$, and temperatures on the order of room temperature $k_B T = 0.01t$, corresponding to ~ 324 K. The dynamical quasiparticle weight Z_n is on the order of unity for all parameters considered here, and the gap equation has a very weak frequency dependence at the values of Ω that have been considered.

The gap enhancement factor Δ'/Δ is shown in Fig. 4. Significant gap enhancement can be seen with a swift rise at intermediate λ , achieving a threefold increase at around $\lambda = 0.8$. The enhancement factor increases slightly with decreasing Δ but is essentially unchanged by modifications to the phonon frequency and temperature for the parameter values used here. I note that there may be some quantitative reduction to this enhancement for the longer-range Fröhlich interaction. Consideration of electron-phonon couplings of up to the order of unity are reasonable since even in metals such as lead, the electron-phonon coupling can be large ($\lambda \sim 1.55$),²⁷ and in the absence of interplane screening, even larger couplings should be possible. Therefore, gap sizes relevant to digital graphene devices should be achievable by placing ionic superstrates on top of, e.g., the graphene-on-rubidium system, and such a system could make a good starting point for experimental investigations of the gap enhancement. It is noted that since

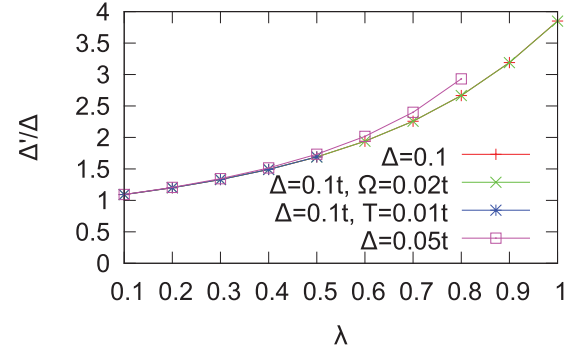


FIG. 4. (Color online) Enhancement of the substrate-induced graphene band gap in the adiabatic (low-phonon-frequency) limit. Gap enhancements of up to a factor of 4 are readily achievable, and for smaller Δ , the gap enhancement is more pronounced at larger λ . Realistic parameters are used: $\Delta = 0.1t$ and $\Delta = 0.05t$, corresponding to bare band gaps of $2\Delta = 0.56$ eV and 0.28 eV, respectively; $t = 2.8$ eV, $\hbar\Omega = 0.01t = 28$ meV, $k_B T = 0.02t = 56$ meV, and $k_B T = 0.01t = 28$ meV, corresponding to $T = 648$ K and 324 K, respectively; and $\lambda \leq 1$. In the plot, $k_B T = 0.02t$ and $\hbar\Omega = 0.01t$ unless otherwise specified. All energy scales are much less than the bandwidth, and changes in T and Ω have only a very small ($<1\%$) effect on the gap. For such a low phonon frequency, the gap function Δ_n has a very weak frequency dependence. The frequency dependence gets even smaller as temperature decreases.

rubidium is a conductor, an insulating material that leads to the same undressed gap would be necessary to make a working digital device. It is possible to rule out a number of materials which have been used for top and bottom gating in transport measurements. I note that gaps can also be induced in bilayer graphene⁷ and graphene nanoribbons,²⁸ so a similar mechanism of substrate-mediated electron-phonon interaction may enhance gaps in those systems.

V. SUMMARY AND CONCLUSIONS

In summary, I have presented a theory for the enhancement of graphene band gaps by polarizable superstrates. The theory predicts gap enhancements of up to fourfold from electron-electron interactions mediated through phonons in a polarizable ionic superstrate. The generation of sizable graphene band gaps is a key problem for the use of graphene in many technologically important applications. The theory shows that the relatively simple addition of polarizable superstrates to graphene systems can provide a way of making large enhancements to graphene gaps. I suggest the following recipe for experimental investigation of an enhanced graphene gap. Form SiO_2 or Si_3N_4 layers on top of graphene on ruthenium intercalated with gold. I note, however, that for digital applications, an insulating substrate is required, so if the effect can be verified experimentally, it will be necessary to find additional substrates that cause gaps in the graphene spectrum. It is hoped that this work will stimulate experiment, leading to tunable gapped graphene systems with applications in digital electronics, LEDs, lasers, and photovoltaics.

ACKNOWLEDGMENTS

I acknowledge EPSRC Grant No. EP/H015655/1 for funding and useful discussions with P. E. Kornilovitch,

A. S. Alexandrov, M. Roy, P. Maksym, E. McCann, V. Fal'ko, N. J. Mason, N. S. Braithwaite, A. Ilie, S. Crampin, and A. Davenport.

-
- ¹S. Y. Zhou, G.-H. Gweon, A. V. Fedorov, P. N. First, W. A. D. Heer, D.-H. Lee, F. Guinea, A. H. C. Neto, and A. Lanzara, *Nat. Mater.* **6**, 770 (2007).
- ²C. Enderlein, Y. S. Kim, A. Bostwick, E. Rotenberg, and K. Horn, *New J. Phys.* **12**, 033014 (2010).
- ³G. Giovannetti, P. A. Khomyakov, G. Brocks, P. J. Kelly, and J. van den Brink, *Phys. Rev. B* **76**, 073103 (2007).
- ⁴A. S. Alexandrov and P. E. Kornilovitch, *J. Phys.: Condens. Matter* **14**, 5337 (2002).
- ⁵M. Steiner, M. Freitag, V. Perebeinos, J. C. Tsang, J. P. Small, M. Kinoshita, D. Yuan, J. Liu, and P. Avouris, *Nat. Nanotechnol.* **4**, 320 (2009).
- ⁶S. Fratini and F. Guinea, *Phys. Rev. B* **77**, 195415 (2008).
- ⁷E. McCann and V. I. Falko, *Phys. Rev. Lett.* **96**, 086805 (2006).
- ⁸E. McCann, D. S. L. Abergel, and V. I. Falko, *Solid State Commun.* **143**, 110 (2007).
- ⁹T. Ohta, A. Bostwick, T. Seyller, K. Horn, and E. Rotenberg, *Science* **313**, 951 (2006).
- ¹⁰Y. Zhang, T.-T. Tang, C. Girit, Z. Hao, M. C. Martin, A. Zettl, M. F. Crommie, Y. R. Shen, and F. Wang, *Nature (London)* **459**, 820 (2009).
- ¹¹M. Fujita, K. Wakabayashi, K. Nakada, and K. Kusakabe, *J. Phys. Soc. Jpn.* **65**, 1920 (1996).
- ¹²K. Nakada, M. Fujita, G. Dresselhaus, and M. S. Dresselhaus, *Phys. Rev. B* **54**, 17954 (1996).
- ¹³M. Y. Han, B. Özyilmaz, Y. Zhang, and P. Kim, *Phys. Rev. Lett.* **98**, 206805 (2007).
- ¹⁴D. V. Kosynkin, A. L. Higginbotham, A. Sinitskii, J. R. Lomeda, A. Dimiev, B. K. Price, and J. M. Tour, *Nature (London)* **458**, 872 (2009).
- ¹⁵C. Tao, L. Jiao, O. V. Yazyev, Y.-C. Chen, J. Feng, X. Zhang, R. B. Capaz, J. M. Tour, A. Zettl, S. G. Louie, H. Dai, and M. F. Crommie, *Nat. Phys.* **7**, 616 (2011).
- ¹⁶J. O. Sofo, A. S. Chaudhari, and G. D. Barber, *Phys. Rev. B* **75**, 153401 (2007).
- ¹⁷D. W. Boukhvalov, M. I. Katsnelson, and A. I. Lichtenstein, *Phys. Rev. B* **77**, 035427 (2008).
- ¹⁸J.-C. Charlier, X. Gonze, and J.-P. Michenaud, *Phys. Rev. B* **47**, 16162 (1993).
- ¹⁹D. C. Elias, R. R. Nair, T. M. G. Mohiuddin, S. V. Morozov, P. Blake, M. P. Halsall, A. C. Ferrari, D. W. Boukhvalov, M. I. Katsnelson, A. K. Geim, and K. S. Novoselov, *Science* **323**, 610 (2009).
- ²⁰S.-H. Cheng, K. Zou, F. Okino, H. R. Gutierrez, A. Gupta, N. Shen, P. C. Eklund, J. O. Sofo, and J. Zhu, *Phys. Rev. B* **81**, 205435 (2010).
- ²¹A. H. MacDonald and R. Bistritzer, *Nature (London)* **474**, 453 (2011).
- ²²L. Covaci and M. Berciu, *Phys. Rev. Lett.* **100**, 256405 (2008).
- ²³A. H. C. Neto, F. Guinea, N. M. R. Peres, K. S. Novoselov, and A. K. Geim, *Rev. Mod. Phys.* **81**, 109 (2009).
- ²⁴J. Hague, P. Kornilovitch, A. Alexandrov, and J. Samson, *Phys. Rev. B* **73**, 054303 (2006).
- ²⁵W. Su, J. Schrieffer, and A. Heeger, *Phys. Rev. B* **22**, 2099 (1980).
- ²⁶I. G. Lang and Yu. A. Firsov, *Zh. Eksp. Teor. Fiz.* **43**, 1843 (1962) [*Sov. Phys. JETP* **16**, 1301 (1963)].
- ²⁷F. Reinert, B. Eltner, G. Nicolay, D. Ehm, S. Schmidt, and S. Hüfner, *Phys. Rev. Lett.* **91**, 186406 (2003).
- ²⁸L. Brey and H. A. Fertig, *Phys. Rev. B* **73**, 235411 (2006).